Numerical Simulation Results of A Lateral Scan Logging Device While Drilling: Analysis of Spatial Resolution

Sudad H Al-obaidi[1]* and Falah H Khalaf[2]

[1]Mining University, SPB, Russia

[2]Oil Exploration Company, Baghdad, Iraq

A B S T R A C T

Formation microimagers are among the most advanced devices used in wireline logging and while drilling. Using three-dimensional numerical modelling, the spatial resolution of the first domestically designed device for lateral scanning logging while drilling (LWD), called the microimager, was assessed. This development marks significant progress in technological capabilities used in oil and gas field developments. An innovative algorithm has been introduced for constructing a geoelectric model that reveals the spatial distribution of specific electrical resistance near the wellbore and opens new possibilities for discoveries. The modelling results indicate that the Lateral logging device offers exemplary spatial resolution, featuring a vertical and azimuthal resolution of 0.10 m, along with a radial depth that exceeds 0.08 m. This high level of precision enhances its effectiveness in data collection and analysis.

Keywords: Numerical simulation; LWD; Microimager; Wellbore; Spatial resolution

Introduction

In recent decades, the number of borehole geophysics methods has grown significantly. Notably, formation micro imagers have emerged, used in wireline logging and during drilling. These devices, instead of traditional logging curves, enable the capture of images—spatial distributions of the measured parameter across the borehole wall[1-5].

In line with import substitution programs, the Research and Production Enterprise of Geophysical Equipment (Luch), together with the A.A. Trofimuk Institute, has developed the "LUCH" hardware complex for logging while drilling[6-10]. The LUCH complex includes a lateral scanning logging (LSL) device, which enables the acquisition of images of apparent electrical resistance (Ra) during drilling. Software based on the finite element method has been developed to calculate the LSL signals[11-14].

This software was utilised to conduct numerical modelling of electrical microimager signals within realistic three-dimensional geoelectric models representing various environments[15,16]. Furthermore, the impact of measurement conditions on the interpretation of imaging results was analysed[17,18]. The potential of using the device to tackle geonavigation challenges was also demonstrated[19,20].

Methodology

The most important characteristic of electrical logging devices is the resolution in assessing the spatial distribution of resistivity[21-25]. In the case of a formation microimager, the spatial resolution of the device is described by three characteristics:

radial depth, vertical and azimuthal resolution[26-30]. To evaluate these device characteristics, a modified classical geoelectric model that includes the well, the invation zone and the formation is used. In the model, the invasion zone is divided into blocks by well depth, z and by azimuthal angle, φ, with each block specifying its resistivity value, $R_{i,j}$ **(Figure 1)**. Such a division, with a small block size, allows for an arbitrary description of the resistivity distribution in the near-wellbore space.
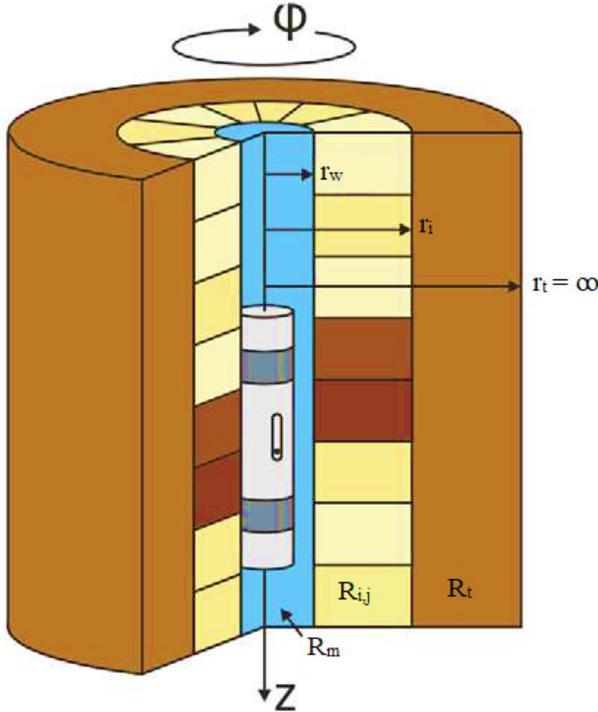

Figure 1: Geoelectric model of the borehole environment for estimating the spatial resolution parameters of the LL device

To estimate the radial depth of the device, geoelectric models are considered in which the invasion zone is uniform and its thickness varies from 0.01 to 0.20 m. The resistivity of the invasion zone (R_i) and the formation resistivity (R_t) range from 3 to 1000 Ohm-meter (Ω·m). In numerical modelling, the following parameters are set: the resistivity of the drilling fluid in the well is 1 Ω·m, the well diameter is 0.220 m and the device diameter is 0.202 m.

The measured signal is expressed as a linear combination of contributions from the invaded zone and the formation:

$$R_a = J(h_i)R_i + [1 - J(h_i)]R_t \qquad (1)$$

In this context, Ra represents the apparent resistivity, while J is a pseudo-geometric factor. This factor serves as a normalized weighting coefficient that quantifies the contributions from both the invaded zone and the formation zone to the measured signal[31-35].

We will define the radial depth of the device as the thickness of the invaded zone (where the pseudo-geometric factor is equal to 0.5.

Results and Discussion

As a result of the modelling, the dependences of the pseudo-geometric factor on the thickness of the invasion zone in geoelectric models at different values of the resistivity of the invasion zone and the formation resistivity were obtained **(Figures 2-4)**.
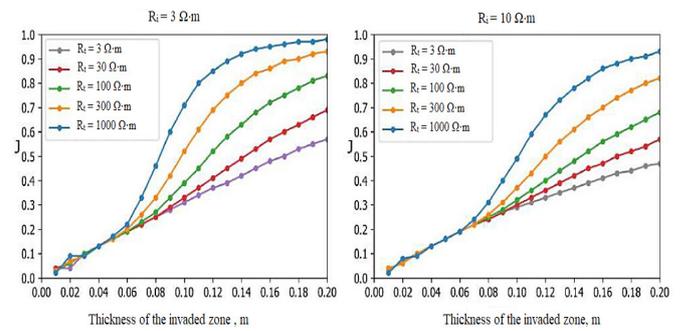

Figure 2: Dependence of pseudogeometric factors on the thickness of the invaded zone, calculated in geoelectric models of the wellbore environment with varying values of Rt and for Ri of 3 and 10 ohm.m

Figure 3: Dependence of pseudogeometric factors on the thickness of the invaded zone, calculated in geoelectric models of the wellbore environment with varying values of Rt and for Ri of 30 and 100 ohm.m.
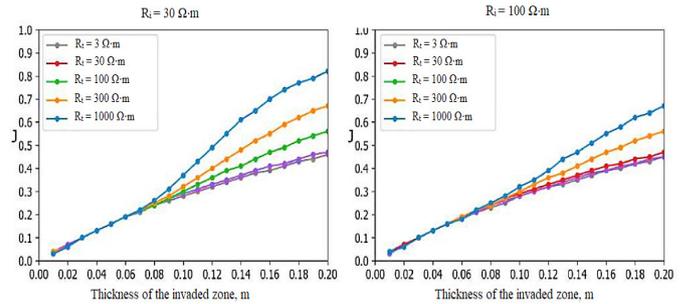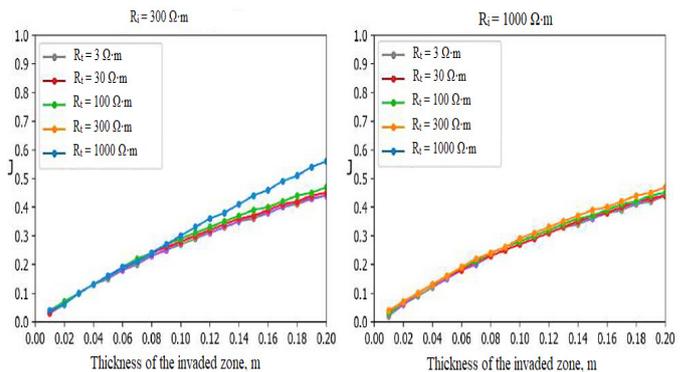

Figure 4: Dependence of pseudogeometric factors on the thickness of the invaded zone, calculated in geoelectric models of the wellbore environment with varying values of Rt and for Ri of 300 and 1000 ohm.m

The simulation results indicate that the radial depth of exploration is primarily affected by the resistivity value of the invasion zone. When the invasion zone resistivity (Ri) is 3 Ohm m, the radial depth varies from 0.08 to 0.17 meters. However, when the resistivity is increased to 1000 Ohm.m, the radial depth exceeds 0.20 meters in all models examined.

To estimate the vertical and azimuthal resolution of the device, a more detailed geoelectric model is employed. In this model, the near-wellbore space is divided into small segments. To determine the resistivity of these segments, an adapted acoustic image is utilised, which reveals cracks of various widths[36-40]. The original image's colors are transformed into shades of gray, with each shade assigned a specific resistivity value ranging from 1 to 2000 Ohm.m **(Figure 5)**. The resulting geoelectric model describes a realistic fractured high-resistivity medium, where the fractures are filled with conductive drilling

fluid. The following parameters are specified for the numerical modelling: the resistivity of the drilling fluid in the well is 1 Ohm·m, the resistivity of the formation is 2000 Ohm·m, the thickness of the invasion zone is 0.50 m, the diameter of the well is 0.220 m, the diameter of the device is 0.202 m, the number of sectors is 16 and the vertical discretisation step is 0.05 m.
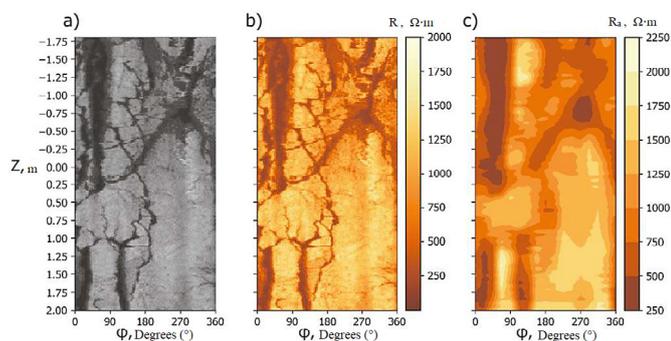

Figure 3: a) High spatial resolution acoustic image, b) Spatial distribution of resistivity in the geoelectric model of the borehole environment, c) Image of apparent resistivity obtained as a result of numerical modelling

Because of the small size of the device's current electrode, its vertical and azimuthal resolutions are each determined by the sampling step along the well depth and the number of azimuthal sectors where measurements are taken. The modelling results indicate that cracks with a width of at least 0.10 m are clearly visible in the image, which corresponds to doubling the sampling step in both the vertical and azimuthal directions.

Conclusions

During the course of this research, an algorithm has been created to facilitate the computation of Lateral Logging (LL) signals within geoelectric models. This algorithm is capable of handling environments characterized by a variety of resistivity distributions in proximity to the wellbore. By accounting for these variations, the algorithm provides more accurate and reliable interpretations of geoelectric data, ultimately enhancing our understanding of subsurface formations. The results of the modelling show that the Lateral logging device has a high spatial resolution: the vertical and azimuthal resolution is 0.10 m and the radial depth exceeds 0.08 m.

Improving vertical and azimuthal resolution involves reducing the measurement sampling step; however, transmitting denser data to the surface in real time is challenging due to the limited bandwidth of the hydraulic communication channel.

References

1. Lai J, Su Y, Xiao L, et al. Application of geophysical well logs in solving geologic issues: Past, present and future prospect. Geoscience Frontiers 2024;15(3):101779.

2. Al-Obaidi SH. Improve the efficiency of the study of complex reservoirs and hydrocarbon deposits - East Baghdad field. Int J Scientific Techno Res 2016;5(8):129-131.

3. Miel H, Hameed AOS, Hussein KF. Modelling and monitoring the development of an oil field under conditions of mass hydraulic fracturing. Trends in Sciences 2022;19(8);3436-3436.

4. Al-Obaidi SH, Khalaf FH. Acoustic logging methods in fractured and porous formations. J Geol Geophys 2017;6(4);2.

5. Chang WJ, Al-Obaidi SH, Patkin AA. Assessment of the condition of the near-wellbore zone of repaired wells by the skin factor. Int Res J Mod Eng Tech Sci 2021;3(4):1371-1377.

6. Nikitenko MN, Epov MI, Glinskikh VN, SuhorukovaKV, Eremin VN. Development of LWD High-frequency Resistivity Tool, Geosciences – Investing in the Future: 6th Saint Petersburg International Conference & Exhibition: proceeding of the conf. (Saint Petersburg, 7 - 10 April 2014), Saint Petersburg, 2014.

7. Al-Obaidi SHA, Chang WJ. Techniques to Boost Oil Production in the Development of Multi-Reservoir Fields. J Earth Environ Waste Manage 2024;2(3):1-7.

8. Smirnov VI, Al-Obaidi S. Innovative methods of enhanced oil recovery. Oil Gas Res 2008;1(e101):1.

9. Al-Obaidi SH. Calculation Improvement of the Clay Content in the Hydrocarbon Formation Rocks. Oil Gas Res 2017;3(1):130.

10. Zhang ZQ, Zhang X, Mu L. Simulation of electromagnetic logging-while-drilling tools using vector finite element methods. IEEE International Symposium on Antennas and Propagation (APSURSI), Spokane, WA, USA, 2011; 2499-2502.

11. Al-Obaidi SH, Patkin AA, Guliaeva NI. Advance Use for the NMR relaxometry to investigate reservoir rocks. J Petrol Eng Technol 2003; 2(3):45-48.

12. Hofmann M, Al-Obaidi SH, Chang WJ. Evaluation of Quantitative Criteria for Triassic Reservoirs in The South Mangyshlak Basin. Natural Sci Advanced Techno Education 2023;32(1).

13. Al-Obaidi SH. Comparison of Different Logging Techniques for Porosity Determination to Evaluate Water Saturation. EngrXiv 1990.

14. Khalaf FH, Al-Obaidi SH. The Effects of Hydro Confining Pressure on the Flow Properties of Sandstone and Carbonate Rocks. Int J Scientific Techno Res 2018;7(2):283-286.

15. Xinxin Qu, Zhanxiang He, Wang Z, et al. Analysis of Oil and Gas Reservoir Prospecting Capability by Borehole-surface Electromagnetic Method Based on 3D Numerical Simulation, SEG Global Meeting Abstracts 2017:1407-1410.

16. Al-Obaidi SH, Chang WJ, Hofmann M. Development Of Oil Fields Using Science Artificial Intelligence and Machine Learning, Natural Sciences and Advanced Technology Education 2023;(32)3-4.

17. Galkin A, et al. Dependences of reservoir oil properties on surface oil. J Pet Eng Emerg 2005; 5(9):74-77.

18. Al-Obaidi SH, Galkin AP. The Assessment of Reservoir Pressure and Recoverable Hydrocarbon Reserves Using Production Well Research Data. J Geol Min 2025; 2(1):1-6.

19. Wang T, Fang S. Investigation of an extra-deep LWD resistivity tool for geosteering and reservoir navigation, SEG Technical Program Expanded Abstracts 2005; 392-395.

20. Al-Obaidi Sudad H. Development of Methodology and Technology for Processing GIS Data. OSF Preprints 1996.

21. Epov MI, Glinskikh VN, Eremin VN, et al. Electromagnetic Tool for High-Resolution Logging: Theoretical and Experimental Studies. Paper presented at the SPE Russian Petroleum Technology Conference 2017.

22. Al-Obaidi SH, Guliaeva NI. Determination of flow and volumetric properties of core samples using laboratory NMR relaxometry. J Petrol Eng Technol 2002;1(2):20-23.

23. Kamensky IP, Al-Obaidi SH. Express study of rheological properties and group composition of oil and condensate using nuclear magnetic resonance-relaxometry. J Oil Gas Coal Technol 2022;4(1):102.

24. Viktor S, Al-Obaidi SH, Khalaf FH. Utilizing Machine Learning to Evaluate the Connection Between Poisson's Ratio and the Petrophysical Properties of Reservoir Rocks. J Petro Chem Eng 2025;1(1):49-54.

25. Al-Obaidi SH, Khalaf FH. Displacement of Reservoir Oil by

Nanoflooding: Physicochemical Mechanisms. J Waste Manag Recycling Tech 2025.

26. Watton T, Cannon S, Brown RJ, Jerram DA, Waichel BL. Using formation micro-imaging, wireline logs and onshore analogues to distinguish volcanic lithofacies in boreholes: examples from Palaeogene successions in the Faroe-Shetland Basin, NE Atlantic. Geological Society 2014;(397):173-192.

27. Hofmann M, Al-Obaidi SH. New Technologies To Investigate The Behaviour Of Silica Gels In Porous Media, Natural Sciences and Advanced Technology Education 2025;34(2).

28. Al-Obaidi SH. Investigation of rheological properties of heavy oil deposits. In Conference of the Arabian J Geosciences. Cham: Springer Int Publish 2019:399-402.

29. Patkin A, Al-Obaidi SH. Influence of Temperature and Pressure of Incoming Oil- Containing Liquid from Field Wells on the Gas Separation Process. J Petro Eng Emerging Techno 2001;(3):20-24.

30. Al-Obaidi SH. Experimental study of the influence of fluid flow rate on the risk of rock destruction. J Pet Eng Emerg Technol 2009;(9):84-89.

31. Merletti G. Assessment of True Formation Resistivity and Water Saturation in Deeply Invaded Tight-Gas Sandstones Based on the Combined Numerical Simulation of Mud-Filtrate Invasion and Resistivity Logs. Petrophysics – The SPWLA Journal of Formation Evaluation and Reservoir Description 2023;(64):502-517.

32. Al-Obaidi SH, Chang WJ, Hofmann M. Development of Oil Fields Using Science Artificial Intelligence and Machine Learning. Natural Sciences and Advanced Technology Education 2023;32(3-4):187-200.

33. Kamensky IP, Al-Obaidi SH, Khalaf FH. Scale effect in laboratory determination of the properties of complex carbonate reservoirs. Int Res J Modernization in Eng Tech Sci 2020;2(11):1-6.

34. Galkin A, Al-Obaidi S, Smirnov V. Numerical Simulation of Water Alternating Gas Injections (WAG) into Hydrocarbon Reservoirs: Factors Influencing Oil Recovery. J Geology Geophysics 2023;12(10):1147.

35. Al-Obaidi SH, Khalaf FH, Alwan HH. Performance analysis of hydrocarbon wells based on the skin zone. Technium 2021;(3):50-56.

36. Meng H, Ye Y, Yang C, Dong D. Study on Rock-Electric Characteristics of Cracked Porous Rocks by the Novel Multifactor Conductivity Model, ACS Omega 2023;8(36):32615-32622.

37. Al-Obaidi S, Smirnov V, Alwan HH. Experimental Study about Water Saturation Influence on Changes in Reservoirs Petrophysical Properties. Walailak J Sci Tech 2021;18(13):1-10.

38. Kamensky IP. The Influence of Permeability Anisotropy on Reservoir Simulation Model Behaviour in Oil Fields. Pet Petro Chem Eng J 2023;7(2):000357.

39. Al-Obaidi SH, Hofmann M. A Study on How Permeability Heterogeneity Influences Initial Water Cut in Undersaturated Oil Formations. Nat Sci Advanced Techno Education 2024;33(5-6).

40. Galkin A, Al-Obaidi S, Smirnov V. Numerical Simulation of Water Alternating Gas Injections (WAG) into Hydrocarbon Reservoirs: Factors Influencing Oil Recovery. J Geology & Geophysics 2023;12(10):1147.